10656 *Biochemistry* **2010,** *49,* 10656–10665
DOI: 10.1021/bi1015452

BIOCHEMISTRY
including biophysical chemistry & molecular biology
Article

Speciated Human High-Density Lipoprotein Protein Proximity Profiles[†]

Kekulawalage Gauthamadasa,[‡] Corina Rosales,[§] Henry J. Pownall,[§] Stephen Macha,[∥] W. Gray Jerome,[⊥] Rong Huang,[‡] and R. A. Gangani D. Silva*[,‡]

[‡]*Department of Pathology and Laboratory Medicine, University of Cincinnati, Cincinnati, Ohio 45237, United States,* [§]*Section of Atherosclerosis and Vascular Medicine, Department of Medicine, Baylor College of Medicine, Houston, Texas 77030, United States,* [∥]*Mass Spectrometry Services, Department of Chemistry, University of Cincinnati, Cincinnati, Ohio 45221, United States, and* [⊥]*Department of Pathology, Vanderbilt University Medical Center, Nashville, Tennessee 37232, United States*

Received September 23, 2010; Revised Manuscript Received November 10, 2010

ABSTRACT: It is expected that the attendant structural heterogeneity of human high-density lipoprotein (HDL) complexes is a determinant of its varied metabolic functions. To determine the structural heterogeneity of HDL, we determined major apolipoprotein stoichiometry profiles in human HDL. First, HDL was separated into two main populations, with and without apolipoprotein (apo) A-II, LpA-I and LpA-I/A-II, respectively. Each main population was further separated into six individual subfractions using size exclusion chromatography (SEC). Protein proximity profiles (PPPs) of major apolipoproteins in each individual subfraction was determined by optimally cross-linking apolipoproteins within individual particles with bis(sulfosuccinimidyl) suberate (BS^3), a bifunctional cross-linker, followed by molecular mass determination by MALDI-MS. The PPPs of LpA-I subfractions indicated that the number of apoA-I molecules increased from two to three to four with an increase in the LpA-I particle size. On the other hand, the entire population of LpA-I/A-II demonstrated the presence of only two proximal apoA-I molecules per particle, while the number of apoA-II molecules varied from one dimeric apoA-II to two and then to three. For most of the PPPs described above, an additional population that contained a single molecule of apoC-III in addition to apoA-I and/or apoA-II was detected. Upon composition analyses of individual subpopulations, LpA-I/A-II exhibited comparable proportions for total protein (∼58%), phospholipids (∼21%), total cholesterol (∼16%), triglycerides (∼5%), and free cholesterol (∼4%) across subfractions. LpA-I components, on the other hand, showed significant variability. This novel information about HDL subfractions will form a basis for an improved understanding of particle-specific functions of HDL.

The anti-atherogenic properties of high-density lipoproteins (HDLs)[1] have made them an attractive target for new therapies against cardiovascular disease (CVD) (*1*, *2*). HDL has antioxidative (*3*) as well as anti-inflammatory properties (*2*) and is a vehicle for reverse cholesterol transport (RCT), which is the transport of cholesterol from the peripheral tissue to the liver for disposal (*1*, *4*). RCT begins with the efflux of cellular cholesterol to lipid free apolipoprotein (apo) A-I via ATP-binding cassette transporter A1 (ABCA1), thereby generating nascent HDL, or to more mature forms of HDL via ABCG1 (*5*−*8*). The compositions and particle sizes of early forms of HDL are modified by plasma lipases, lipid transfer proteins, and lecithin:cholesterol acyltransferase (LCAT), which converts nascent discoidal HDL to spherical HDL (*6*, *9*−*12*). The neutral lipid content in HDL is modified by cholesteryl ester transfer protein (CETP)-mediated exchange of their cholesteryl esters (CE) for triglycerides (TG) in the very low-density lipoprotein (VLDL) (*10*, *13*). This remodeling generates a heterogeneous mixture of HDL particles with different sizes, shapes, and apolipoprotein:lipid ratios.

Although recent studies have identified more than 100 proteins associated with human HDL (*14*, *15*), and these HDL-associated proteins have been shown to be subfraction-specific (*16*), the majority of HDL proteins are apoA-I (∼70%) and apoA-II (∼20%) (*17*). The remainder of the proteins are mainly composed of apoC's (mainly apoC-III, ∼2−4%), apoD, and apoE (< 2%) (*17*, *18*). From these compositional data, one can infer that many HDL-associated proteins are minor components, perhaps only transiently present during functional interactions and remodeling processes. Thus, the major HDL apolipoproteins are most likely the most important but not the sole determinants of HDL composition, particle size, and functionality. Moreover, the distinct apolipoprotein compositions of HDL subfractions are expected to control their metabolic fates.

HDL occurs as LpA-I, which contains apoA-I but not apoA-II, and LpA-I/A-II, which contains both apoA-I and apoA-II (*19*, *20*). The interactions of LpA-I/A-II and LpA-I with plasma factors are different, indicating that apoA-II modulates the effects of apoA-I (*21*−*23*). Although high plasma levels of

[†]The work was supported by grants from the National Institutes of Health to R.A.G.D.S. (National Heart, Lung and Blood Institute Grant HL087561) and H.J.P. (Grants HL030914 and HL056865).

*To whom correspondence should be addressed. Phone: (513) 558-4325. Fax: (513) 558-1312. E-mail: silvar@ucmail.uc.edu.

[1]Abbreviations: apo, apolipoprotein; ABCA1, ATP-binding cassette transporter A1; βME, β-mercaptoethanol; BS^3, bis(sulfosuccinimidyl) suberate; CC, covalent chromatography; CE, cholesteryl ester; CETP, cholesteryl ester transfer protein; DTT, dithiothreitol; FC, free cholesterol; HDL, high-density lipoprotein; fr, fraction number; LCAT, lecithin:cholesterol acyltransferase; LpA-I, HDL with apoA-I but without apoA-II; LpA-I/A-II, HDL with apoA-I and apoA-II; M_r, molecular mass; PBS, phosphate-buffered saline; PC, phosphatidylcholine; PL, phospholipids; PPP, protein proximity profile; RCT, reverse cholesterol transport; rHDL, reconstituted HDL; SEC, size exclusion chromatography; STB, standard Tris buffer; TBS, Tris-buffered saline; TFA, trifluoroacetic acid; TC, total cholesterol; TG, triglycerides; ToF, time of flight; TP, total protein; TPS, thiopropyl Sepharose; VLDL, very low-density lipoprotein.

 Published on Web 11/12/2010

apoA-II are associated with a lowered risk of CVD events (*24*, *25*), there is little understanding about beneficial functions of apoA-II. Furthermore, structurally, even the molecular stoichiometry of apoA-I and apoA-II in individual HDL particles or segregation of other apolipoproteins into specific native HDL particles is not known. Such information would provide a basis for further insights into the functional consequences of these individual particles. It is clear that the LpA-I and LpA-I/A-II main populations undergo different metabolic processes. These include their sites of generation (*26*, *27*), different interaction capabilities with various plasma factors (*21*−*23*), and catabolism (*28*). In the context of their heterogeneity, several methods have been used to determine HDL:apolipoprotein stoichiometry, including immunonephelometry (*29*, *30*) and cross-linking followed by gel-based interpretations (*31*). The former method measures scattered light intensity as a function of particle size, and the stoichiometries are then estimated compared to standards with known compositions (*29*, *30*). The latter method determines the migration distance of cross-linked HDL particles by sodium dodecyl sulfate−polyacrylamide gel electrophoresis (SDS−PAGE), and the molecular mass (M_r) determinations of these complexes are conducted with respect to a set of M_r standards. This method has been widely used to determine the number of apolipoprotein molecules in HDL (*26*, *32*−*34*). Streaking of the gel bands, due to variability in cross-linker addition, and unpredictable gel band migration, due to location of cross-linker formation in the protein sequence, render this method less than optimal for determining apolipoprotein stoichiometry (*33*). We developed a method combining cross-linking chemistry with MALDI-MS that, unambiguously, determines the number of apolipoprotein molecules in reconstituted HDL (rHDL) particles (*35*). The stoichiometry of proximal apolipoproteins can be determined using this method based on the absolute masses of the cross-linked apolipoproteins. The method uniquely qualifies for this purpose, has moderate sensitivity, and hence is capable of capturing only the most abundant apolipoproteins present in HDL. To date, methods used to detect HDL apolipoproteins, including liquid chromatography and mass spectrometry (LC−MS), have not demonstrated the ability to determine molecular stoichiometries of apolipoproteins in HDL.

Here, we report, for the first time, apolipoprotein protein proximity profiling (PPP), average particle diameters, and apoprotein:lipid stoichiometries in native LpA-I and LpA-I/A-II isolated from human plasma. We have used a unique set of chromatographic techniques to first separate HDL into LpA-I and LpA-I/A-II followed by the separation of each of these main pools into six individual subfractions (Figure 1). Cross-linking, followed by the application of the MALDI-MS technique optimized for native HDL, demonstrated clear differences in the size, composition, and number of major apolipoproteins in LpA-I versus LpA-I/A-II. Our studies have also highlighted a unique distribution of apoC-III among different HDL subfractions.

EXPERIMENTAL PROCEDURES

Isolation of HDL from Human Plasma. HDL was isolated from pooled-fresh human plasma upon sequential flotation at density values of 1.063 and 1.21 g/mL as described previously (*36*, *37*). Plasma was obtained within 2 days of blood draw, from the Hoxworth Blood Bank (Cincinnati, OH).

Separation of HDL into LpA-I and LpA-I/A-II. Total HDL was separated into LpA-I and LpA-I/A-II subpopulations with the use of covalent chromatography (CC) incorporating

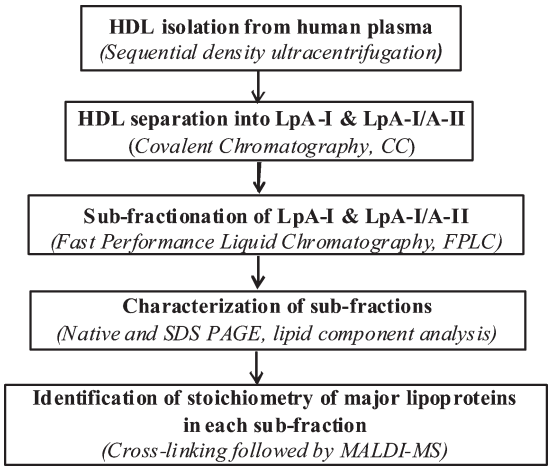

FIGURE 1: Main experimental steps and techniques used in the study.

Thiopropyl Sepharose beads (TPS) (GE Healthcare, Piscataway, NJ) (*38*). See the Supporting Information for method details.

LpA-I and LpA-I/A-II Subfractionation. Individual LpA-I and LpA-I/A-II pools were further separated on the basis of the average particle size by size exclusion chromatography (SEC) using two Superose 6 HR columns (GE Healthcare) connected in tandem. Particle separation was conducted via introduction of 10 mg of total protein in 250 μL into the column setup, operated at a flow rate of 0.4 mL/min. Each elution profile was divided into six subfractions, based on the elution volume, with fraction 1 (fr 1) having the shortest elution time (hence the largest average particle size) and fr 6 having the longest elution time (hence the smallest average particle size). LpA-I/A-II and LpA-I subfractions with a common fraction number correspond to the same elution volume in the chromatographic profiles. In a specific case (see Discussion), 0.5 mg of total HDL protein was separated on four sizing columns connected in tandem (three Superdex 200 columns followed by a single Superose 6 column).

Cross-Linking of HDL Subfractions and Processing for MALDI-MS. All subfractions were cross-linked with a 1:100 total protein:cross-linker bis(sulfosuccinimidyl) suberate (BS^3) molar ratio at a total protein concentration of 1 mg/mL. Please see the Supporting Information for method details, including additional cross-linker use, delipidation, and sample processing for MALDI.

MALDI-MS Measurements and Spectral Processing. The measurements were carried out as before with few modifications (*35*). See the Supporting Information for details. Spectral comparisons were conducted using MoverZ (Genomic Solutions, Ann Arbor, MI). Spectra were subjected to 50% Fourier smoothing and normalized to the same height using the most intense cross-linked mass peak in the spectrum within the 50−130 kDa range, using Grams 32 (Galactic Industries, Salem, NH).

Lipid Component Analysis. Amounts of total cholesterol (TC), free cholesterol (FC), total protein (TP), triglycerides (TG), and phospholipids (PL) in each subfraction were determined enzymatically (Wako Diagnostics, Richmond, VA) according to the manufacturer's instructions on a Bio-Tech synergy HT microplate reader.

Gel Electrophoresis. Phast gradient gels (from 8 to 25%) were purchased from GE Healthcare along with the high- and low-molecular mass standards (catalog numbers 17-0445-01 and 17-0446-01, respectively); 4 to 30% gradient gels were cast in our laboratory. The diameter or the M_r of the cross-linked complexes

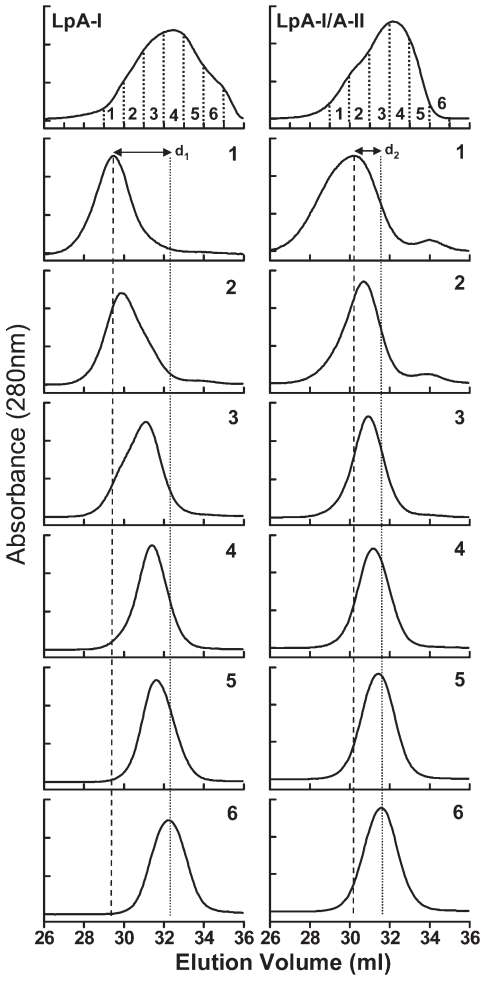

FIGURE 2: Size exclusion chromatography of LpA-I and LpA-I/A-II. Chromatographic traces of LpA-I and LpA-I/A-II upon separation on two Superose 6 columns connected in tandem (top). Each main pool was divided into six individual subfractions based on the elution volume and was numbered from 1 to 6. The individual chromatography profile of each subfraction is shown below the corresponding main pool. The distances between the largest average particle size and the smallest average particle size are shown by d_1 for LpA-I and d_2 for LpA-I/A-II. The average sizes of the largest and smallest particles are shown by vertical short dash and long dash lines, respectively.

was calculated by comparison of their migration distances with those of the standards.

Electron Microscopy Measurements. See the Supporting Information for methods used in EM measurements.

RESULTS

Native HDL Subfractionation and Characterization. The SEC profiles of LpA-I, LpA-I/A-II, and the six individual subfractions generated thereof are shown in Figure 2. LpA-I and LpA-I/A-II fractions with the same numbers, have the same elution volumes. As expected, these subfractions clearly indicated a decrease in the average particle diameters from fr 1 to fr 6. The shift in the average particle diameter for LpA-I (indicated by d_1) is larger than that for LpA-I/A-II (d_2). This observation indicates that variation in the particle size was larger in LpA-I than in LpA-I/A-II, which was confirmed with other independent HDL pools (data not shown).

On the basis of SDS−PAGE performed under nonreducing conditions, all LpA-I/A-II subfractions contained predominantly large amounts of apoA-II (>90%) compared to LpA-I, thereby

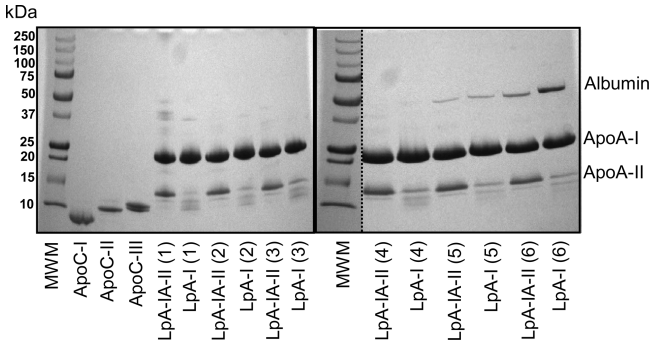

FIGURE 3: Major apolipoproteins in LpA-I and LpA-I/A-II subfractions as visualized by SDS−PAGE. LpA-I and LpA-I/A-II subfractions (adjusted to 1 mg/mL total protein concentration) on 4 to 30% SDS-PAGE. ApoA-I and apoA-II band locations as well as albumin contamination (prevalent in LpA-I fr 6) are indicated. ApoC-I, apoC-II, and apoC-III standards are included. Lanes with molecular mass standards are denoted as MWM. Gels were stained with Coomassie Blue.

confirming effective separation of LpA-I from LpA-I/A-II (Figure 3). In addition to apoA-I and apoA-II, additional bands corresponding to proteins with lower M_r values were observed and were prominent in LpA-I (Figure 3). Comparison with apoC standards (apoC-I, apoC-II, and apoC-III) indicated that these proteins were likely apoC-III_1 and apoC-III_2, the two major isomeric forms of apoC-III (*39*). Others have reported the third most abundant HDL apolipoprotein to be apoC-III, making up ~2−4% of total HDL proteins (*17*, *39*). Moreover, serum albumin was specifically present in the smallest subfractions of LpA-I and LpA-I/A-II (fr 6). The identities of apoA-I, apoA-II, albumin, and apoC-III were confirmed by MALDI-ToF/ToF analysis, upon gel band extraction followed by tryptic digestion (data not shown). Moreover, on the basis of PAGE determinations and MALDI/ToF/ToF, we were able to confirm the presence of apoD (29 kDa major, 38 kDa minor) and apoE (35 kDa) in LpA-I/A-II fr 1 [Figure 3, lane 1 (LpA-I/A-II)] with the identification of 2 and 7 protein specific peptides respectively. However, sequence evidence for the minor M_r band at ~37 kDa in lane 1 of LpA-I was not found.

SDS−PAGE of cross-linked LpA-I and LpA-I/A-II subfractions revealed products with different migration patterns (Figure 4). The protein:cross-linker ratio of 1:100 was previously shown to be sufficient to almost fully cross-link proximal proteins within the cross-linker spacer arm length, 11.4 Å, in discoidal rHDL particles (*35*). However, in native HDL, a small fraction of apoA-I did not form intermolecular cross-links, implying that a fraction of apoA-I might be in an orientation that cannot be cross-linked. Even though cross-linked subfractions appeared as smeared bands on SDS-PAGE, a few prominent condensed bands could be pin-pointed for LpA-I and LpA-I/A-II (indicated by arrows in Figure 4). For LpA-I, these bands are located at ~52 (a), 69 (b), 97 (c), and 152 kDa (d), while for LpA-I/A-II, they are located near 70 (m), 88 (n), 97 (o), and 145 kDa (p). The 69−70 kDa (b and m) bands correspond to internally cross-linked albumin and are outside the range of cross-linked complexes of LpA-I/A-II, but within the range of cross-linked masses for LpA-I. The apparent range of cross-linked masses across all six subfractions is larger for LpA-I than for LpA-I/A-II. However, exact mass ranges cannot be evaluated because of the broad streaking nature of the gel bands. Albumin migrated as a free protein, as seen by 8 to 25% Native PAGE

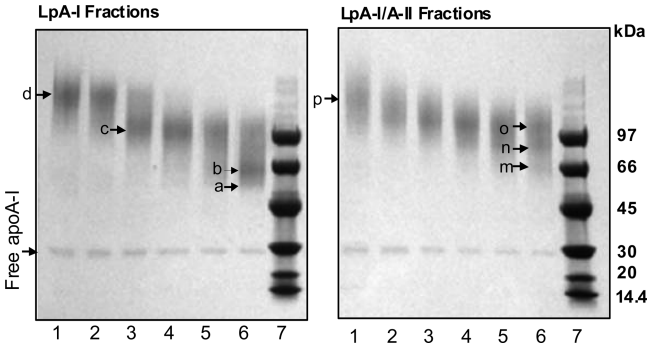

FIGURE 4: SDS−PAGE of cross-linked LpA-I and LpA-I/A-II subfractions. Individual subfractions of LpA-I and LpA-I/A-II were cross-linked at a 1:100 total protein:BS^3 cross-linker ratio at 1 mg/mL protein and were subjected to 4 to 15% SDS−PAGE. Band b in lane 6 (left panel) and band m in lane 6 (right panel) correspond to albumin contamination (~66 kDa). The small amount of apoA-I that was not involved in intermolecular cross-linking is shown as Free apoA-I. Labeling of fractions is similar to Figures 2 and 3. Low-molecular mass (LMW) markers are in lane 7. Gels were stained with Coomassie Blue.

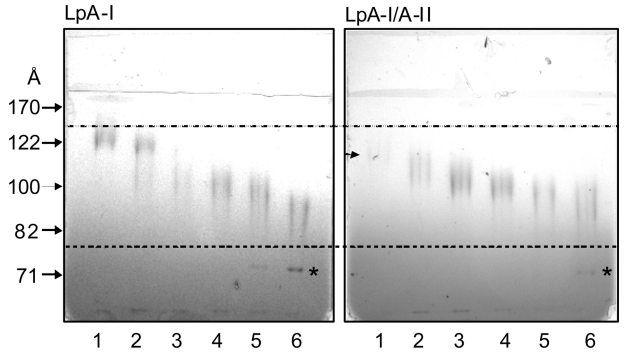

FIGURE 5: Native PAGE characterization of cross-linked LpA-I and LpA-I/A-II. Individual cross-linked LpA-I and LpA-I/A-II subfractions (at a total protein concentration of 1 mg/mL) used in Figure 4 were subjected to 8 to 25% Native PAGE. The locations of the hydrodynamic diameters of the high-molecular mass markers are indicated by arrows. The numbering of the subfractions is similar to Figures 2−4. The location of LpA-I/A-II fr 1, which is not clear on the gel, is marked with an arrow. The locations of the internally cross-linked albumin in fr 6 of LpA-I and LpA-I/A-II pools are marked with asterisks. Gels were stained with Coomassie Blue.

[Figure 5, lane 6 (LpA-I and LpA-I/A-II)]. This confirmed that albumin was present as a free contaminant protein and was not associated with HDL, contrary to what was predicted previously (*40*). On the basis of the migration distances of cross-linked subfractions on Native PAGE, the average particle diameters for LpA-I and LpA-I/A-II ranged from 78 to 126 Å and from 85 to 110 Å, respectively (Figure 5). These dimensions are likely smaller than the actual hydrodynamic diameters because cross-linking is known to reduce the apparent particle diameters. Native PAGE of non-cross-linked subfractions at a total protein concentration of 1 mg/mL did not provide useful information because complexes fell apart during electrophoresis (data not shown). Even though this could have been avoided by running samples at high total protein concentrations of ≥4 mg/mL (*16*), we decided to maintain the concentration of 1 mg/mL (standard physiological concentration for apoA-I) throughout the experiments.

PPPs of LpA-I and LpA-I/A-II Subfractions. The results of MALDI-MS of cross-linked LpA-I and LpA-I/A-II subfractions are shown in Figure 6. This MS technique has the ability to

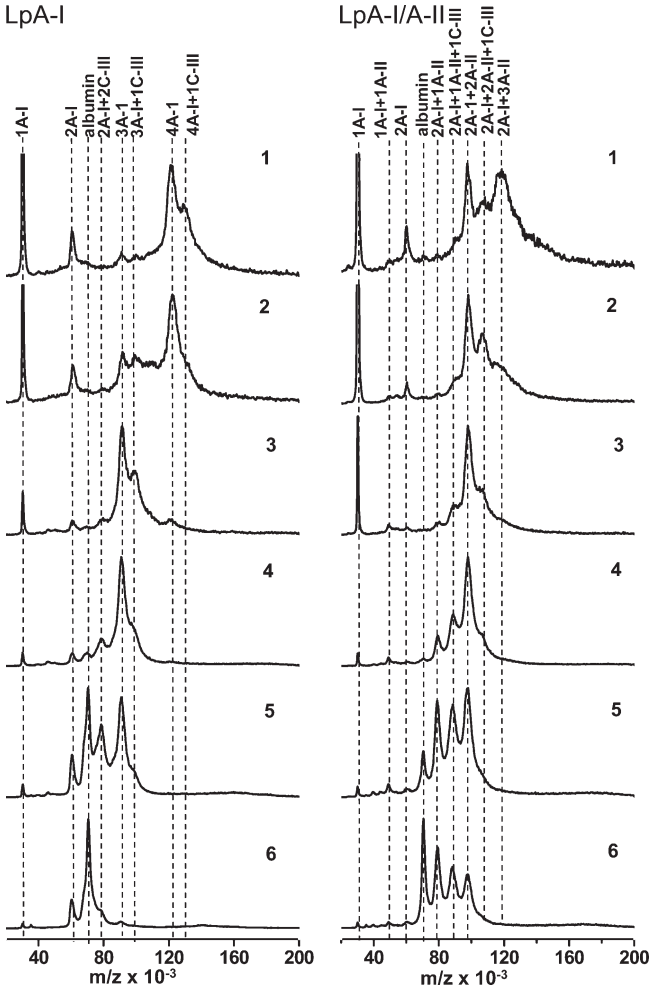

FIGURE 6: MALDI mass spectra of cross-linked LpA-I and LpA-I/A-II subfractions. Individual cross-linked subfractions (shown in Figures 4 and 5) were subjected to MALDI-MS measurements in the 10−200 kDa range. Possible combinations of apolipoproteins that can be attributed to major peaks in the MALDI spectrum are indicated above the vertical dotted lines that connect similar M_r values in each spectrum. The peak location that corresponds to the albumin contamination is indicated as albumin.

ionize and generate singly charged ions that can be assigned directly to the M_r of the cross-linked complexes. All spectra were normalized to a peak height of 1, using the most intense cross-linked peak in the spectrum. One of the major observations seen in MALDI spectra is that subfractions from both main pools show an average M_r shift toward higher masses when going from the smallest (fr 6) to the largest (fr 1) subfraction. This implies that the larger particles have more apolipoprotein molecules per particle as seen by PAGE (Figure 4). However, unlike SDS−PAGE results, each MALDI spectrum consisted of a set of resolved multiple peaks for which M_r can be determined within ~50 Da. Mass peaks in these spectra have originated from optimally cross-linked subfractions and hence consisted of intermolecularly cross-linked apolipoproteins within each HDL particle in a subfraction. Multiple peaks in each spectrum indicated the presence of multiple particle populations within a subfraction.

Under our cross-linking conditions, 1:100 total protein:BS^3 ratio, small LpA-I and LpA-I/A-II subfractions (fr 6, 5, 4) were fully cross-linked as seen by the diminution or the absence of a peak corresponding to free apoA-I (1A-I). However, upon going from smaller to larger subfractions, we found the peaks

Table 1: Assignments of MALDI-MS Peaks to the Most Abundant HDL Apolipoproteins and Their Combinations

	calculated M_r (kDa)[a]	predicted MALDI-MS mass (kDa)[b]	presence in MALDI-MS[c]	clarity by MALDI-MS	clarity by MALDI-MS and PAGE
1A-I[d]	**28.1**	**30.3**	**yes (*30.3*)**	**yes**	**yes**
1A-I+1C-III	36.9	39.8	no	n/a[e]	n/a[e]
1A-I+1A-II	45.5	49.1	yes (*49.1*)	yes	yes
2A-I[d]	**56.2**	**60.6**	**yes (*60.6*)**	**yes**	**yes**
1A-I+2A-II	62.9	67.9	no	n/a[e]	n/a[e]
2A-I+1C-III	65.0	70.2	yes (*70.4*)	no	partial
albumin	66.4	71.7	yes (*70.4*)	no	partial
2A-I+1A-II	73.6	79.5	yes (*78.9*)	no	partial
2A-I+2C-III	73.6	79.5	yes (*78.3*)	no	partial
2A-I+1A-II+1C-III	82.4	88.9	yes (*88.7*)	yes	yes
3A-I[d]	**84.3**	**91.1**	**yes (*91.1*)**	**yes**	**yes**
2A-I+2A-II	91.0	98.3	yes (*97.8*)	yes	yes
3A-I+1C-III	93.0	100.5	yes (*98.9*)	yes	yes
2A-I+2A-II+1C-III	99.8	107.8	yes (*105.6*)	yes	yes
3A-I+1A-II	101.7	109.9	no	n/a[e]	n/a[e]
3A-I+2C-III	101.7	109.9	no	n/a[e]	n/a[e]
2A-I+3A-II	108.4	117.4	yes (*117.6*)	yes	yes
4A-I[d]	**112.4**	**121.5**	**yes (*121.1*)**	**yes**	**yes**
3A-I+2A-II	119.1	128.7	no	n/a[e]	n/a[e]
4A-I+1C-III	121.15	130.9	yes (*129.5*)	yes	yes
5A-I[d]	**140.5**	**151.9**	**no**	**n/a[e]**	**n/a[e]**
4A-I+1A-II	147.2	159.1	no	n/a[e]	n/a[e]

[a]Masses of apolipoprotein combinations were calculated by addition of theoretical M_r values of the corresponding apolipoproteins. [b]Predicted MALDI-MS peak locations for cross-linked apolipoproteins in LpA-I and LpA-I/A-II subfractions were estimated on the basis of the linear regression obtained for lipid free apoA-I measurements (Figure 7). A linear regression was generated between theoretical masses for apoA-I monomer, dimer, trimer, tetramer and observed MALDI-MS masses for optimally cross-linked apoA-I oligomers, which resulted in a correlation coefficient of 0.99. [c]The presence of the predicted masses in MALDI-MS spectra is indicated as yes or no along with the observed masses in parentheses. [d]Predicted masses for the rows highlighted in bold were taken directly from the cross-linked apoA-I oligomer measurements in Figure 7. [e]Not applicable.

corresponding to monomeric apoA-I (1A-I) and cross-linked dimeric apoA-I (2A-I) were more prominent in the spectrum compared to the cross-linked complex (fr 2 and fr 1). Because the cross-linking conditions were optimized for rHDL particles (*35*), we took steps to confirm that partial cross-linking was not due to an insufficient protein:cross-linker ratio used in native HDL. To test this, we cross-linked total HDL as a function of increasing protein:BS^3 ratio from 1:100 to 1:400 and recorded the spectra (data not shown). A 3-fold increment in the amount of BS^3 did not change the peak height of the monomeric apoA-I that escaped intermolecular cross-linking, meaning the peak corresponding to apoA-I was not due to insufficient cross-linking (data not shown). Moreover, increasing the spacer arm length from 7.7 Å (DSG) to 16.1 Å (Sulfo-EGS) did not affect the MS peak height for monomeric apoA-I.

The increase in the amounts of monomeric apoA-I in larger subfractions seen by MALDI was not apparent on PAGE (Figure 4). To test whether monomeric apoA-I ionization would be suppressed when dimeric apoA-I was present (a situation representative of small particles), we cross-linked rHDL that contained exactly two molecules of apoA-I at different protein:cross-linker ratios (from 1:10 to 1:100). The presence of the apoA-I dimer did not suppress monomeric apoA-I ionization (data not shown). On the basis of this observation, it can be suggested that the amount of lipid free apoA-I was negligible in smaller subfractions despite less variability seen on the gel.

We assigned the major MALDI-MS peaks to a single HDL apolipoprotein or combinations of the most prevalent HDL apolipoproteins, whose presence and abundance were confirmed by SDS−PAGE of non-cross-linked subfractions (Figure 3). The observed MALDI-MS peaks for cross-linked subfractions shifted from the calculated masses generated by the addition of molecular masses of apolipoproteins, because of the presence of cross-links in the complex (Table 1). For example, every addition of cross-linker BS^3 resulted in a 138.1 Da increment in the mass of the complex. The mass shifts for different apolipoprotein combinations were predicted on the basis of the M_r shifts observed for the cross-linked lipid free apoA-I peaks in MALDI-MS (Figure 7). Lipid free apoA-I was processed similar to native HDL subfractions by cross-linking in PBS with a 1:100 protein:BS^3 molar ratio (Figure 7A). The linear regression between theoretical M_r values for apoA-I oligomers and experimentally observed apoA-I MALDI-MS peaks correlated with a regression coefficient of 0.99. The equation representing the linear fit (Figure 7B) was used to predict the MALDI-MS M_r values for major apolipoprotein combinations (Table 1, predicted MALDI-MS). Theoretical addition of M_r for individual apolipoproteins (calculated M_r), their predicted MALDI-MS, and the observed MALDI-MS peaks are reported in Table 1. Except for two peaks, which could not be assigned to a single apolipoprotein combination because of the presence of two possibilities, clear assignments could be given to all the other peaks.

The PPPs of small subfractions of LpA-I indicated two apoA-I molecules (2A-Is, fr 6 and fr 5) and three apoA-I molecules (3A-Is, fr 5 and fr 4) per particle. Because there is no peak corresponding to 1A-I in these spectra, we suggest that the peak for 2A-I is not a result of partial cross-linking. Moreover, LpA-I/A-II lacking a peak corresponding to 2A-I, further supported this interpretation and confirmed the high quality of separation of LpA-I/A-II from LpA-I. With increasing subfraction size, (fr 3 to fr 1), free apoA-I (1A-I) due to incomplete cross-linking was seen. These PPPs indicated that LpA-I had mainly 3A-Is and 4A-Is per particle (fr 2 and fr 1). While LpA-I had a quantized increase in

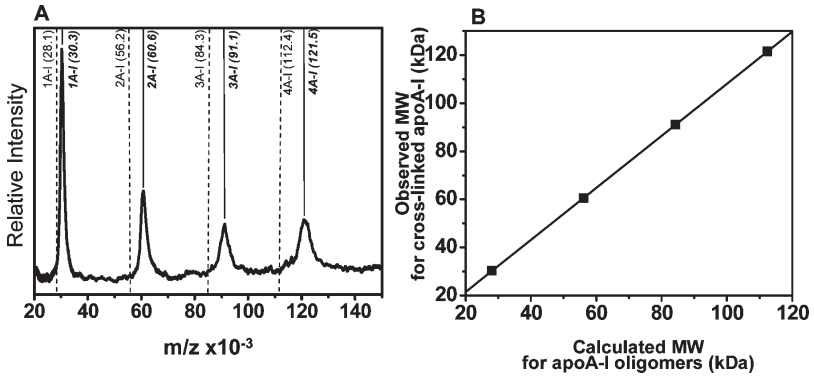

FIGURE 7: Linear regression between theoretical masses for oligomeric apoA-I vs observed masses for cross-linked apoA-I. (A) MALDI-MS of self-associated lipid free apoA-I upon cross-linking with BS^3 at a 1:100 protein:BS^3 molar ratio with the peak locations marked by solid lines and masses given in parentheses in italics. Predicted M_r values for non-cross-linked oligomers are shown by dashed lines along with corresponding M_r values in parentheses. (B) Linear regression of predicted vs observed M_r values given in panel A.

the number of apoA-I molecules with increasing particle size, namely, 2A-I (fr 6 and fr 5), 3A-I (fr 4 and fr 3), and 4A-I (fr 2 and fr 1), the combination 2A-I+2A-II dominated all six LpA-I/A-II subfractions (Figure 6). In addition to this predominant particle, the smallest LpA-I/A-II subfraction had an additional peak, representing 2A-I+1A-II (fr 6 and fr 5), while the largest subfractions had 2A-I+3A-II (fr 1). In large LpA-I/A-II subfractions, the spectra indicated incomplete cross-linking, as seen for LpA-I large fractions (fr 3, 2, 1).

There were cross-linked species containing one apoC-III molecule in each population, including 3A-I+1C-III and 4A-I+1C-III. However, the presence of 2A-I+1C-III was precluded by overlap with an albumin contamination (Table 1 and Figure 6). Nevertheless, Native PAGE of this subfraction indicated the presence of a HDL complex, not just free albumin, hinting at the possible presence of 2A-I+1C-III. As observed for LpA-I, PPPs of each of the LpA-I/A-II subfractions were indicative of having particles with 2A-I+1A-II+1C-III and 2A-I+2A-II+1C-III. Because of the trailing of the spectral peaks for LpA-I/A-II (fr 1) above 120 kDa, the presence of a particle population with 2A-I+3A-II+1C-III was not clearly detectable (Figure 6). The presence of apoD and apoE preferentially in this LpA-I/A-II subfraction added to the complications of our interpretations [Figure 3, lane 1 (LpA-I/A-II)].

Lipid Composition. The lipid compositions (i.e., PL, TC, FC, and TG) and the percentage of total protein of LpA-I and LpA-I/A-II were comparable to those reported for total HDL (*41*). The smaller LpA-I and LpA-I/A-II subfractions had similar lipid compositions (Figure 8). However, in larger subfractions, there were statistically significant differences between LpA-I and LpA-I/A-II for all lipid components and total protein. Consistently, the percentages of PL, FC, and TC were higher in larger LpA-I fractions than in LpA-I/A-II fractions. On the other hand, the percentages of total protein and TG contents were significantly lower in the larger LpA-I subfraction than in the LpA-I/A-II subfraction. Another remarkable difference between LpA-I and Lp-I/A-II subfractions was the compositional uniformity of LpA-I/A-II compared to LpA-I, across all six subfractions. This agreed with the more uniform particle sizes for the former (Figure 5) and less variability in the composition of LpA-I/A-II.

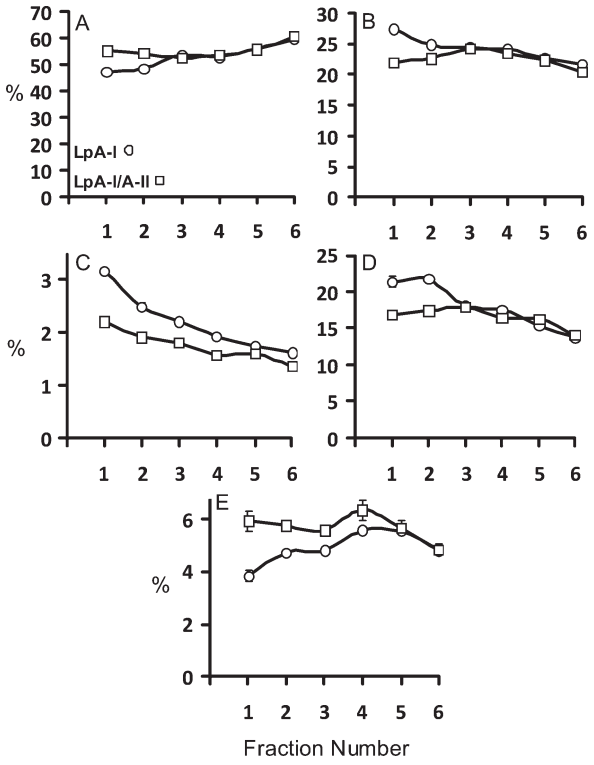

FIGURE 8: Main lipid and total protein compositional analysis of individual LpA-I and LpA-I/A-II subfractions. Total protein and lipid component analyses were conducted using WAKO chemical kits. The components are presented as mass percentages for individual subfractions. The subfraction labeling is similar to Figures 2−6: (A) total protein, (B) phospholipids, (C) free cholesterol, (D) total cholesterol, and (E) triglycerides.

DISCUSSION

Major Outcomes. Our measurements on LpA-I and LpA-I/A-II separated by size unambiguously supported the presence of LpA-I with two, three, and four molecules of apoA-I per particle. In contrast, all LpA-I/A-II subfractions contained only two molecules of apoA-I per particle, supporting the concept that apoA-II had the ability to displace apoA-I from HDL (*42*, *43*). The number of dimeric apoA-II molecules in LpA-I/A-II subfractions varied from one to two to three. Prior reports indicated that up to two-thirds of total HDL was LpA-I/A-II (*20*, *38*, *44*). Our data, collected on independent plasma batches, not only confirmed that approximately two-thirds of HDL was LpA-I/A-II but also revealed that the predominant LpA-I/A-II particle was 2A-I+2A-II. All LpA-I/A-II subfractions, having nearly uniform particle sizes, protein contents, and major lipid components compared to those of quantized LpA-I particles, indicated

extensive size rearrangements of large and small LpA-I upon apoA-II incorporation or direct incorporation of apoA-II onto midsized LpA-I particles. Moreover, our data indicated a uniform distribution of apoC-III across all subfractions irrespective of particle size, opposing prior interpretations (Figure 6) (*45*). On the other hand, our analyses indicated the predominant presence of apoD and apoE on a specific subfraction of LpA-I/A-II (Figure 3). Subfractions containing larger LpA-I particle populations consisted of higher TC and FC contents than as well as estimated amounts of CE compared to LpA-I/A-II (Figure 8), indicating that these particles could be better mediators of the RCT pathway.

Method Optimization. The major obstacle, in compositional analysis of native HDL, is the presence of multiple particle populations with different combinations of apolipoproteins (*19*). Application of MALDI-MS on cross-linked total HDL generated broad overlapping peaks with the most intense peak consistently centered at ~98 kDa, originating mainly from 2A-I+2A-II (data not shown). Our separation techniques reduced the complexity of total HDL and generated subfractions with manageable apolipoprotein heterogeneity for downstream analyses. Another challenge was the delipidation of native cross-linked subfractions, for which stringent delipidation conditions were required compared to those for rHDL, for obtaining clean MS peaks (see Experimental Procedures). Furthermore, we took precautions to prevent false detection of noncovalent mass assemblies and aggregates of apolipoprotein molecules, which could be misinterpreted as a single cross-linked oligomeric entity by MALDI-MS. This was conducted via optimization of the laser power during spectral acquisitions on bovine serum albumin (BSA; M_r = 66.0 kDa), and unmodified apoA-I (M_r = 28.1 kDa), until there were no observable oligomeric aggregates (i.e., two, three, and four noncovalently bound molecules carrying a single charge, $2MH^+$, $3MH^+$, and $4MH^+$, respectively).

Molecular Stoichiometry. The presence of HDL particles containing two to three molecules of apoA-I in the highest-density subfraction (HDL_{3c}) and four to five molecules of apoA-I in the lowest-density subfraction (HDL_{2b}) has been reported (*41*). In addition, prior studies on HDL subfractions isolated by density followed by cross-linking and gel-based methods have estimated the presence of LpA-I particles with at least two, three, and four molecules of apoA-I per particle (*40*, *46*, *47*). Consistent with these findings, in vitro spherical rHDL generated by incubation of discoidal rHDL with LCAT alone and LCAT followed by CETP were reported to contain three and two apoA-I molecules per particle, respectively (*32*, *48*). Former studies of LpA-I/A-II, isolated by density subfractionation followed by immunoaffinity chromatography, have reported an average apoA-I:apoA-II molar ratio that ranges from 1:1 to 2:1 in LpA-I/A-II (*20*, *47*, *49*). For LpA-I/A-II, we detected three different particle types, 2A-I+1A-II, 2A-I+2A-II, and 2A-I+3A-II, with 2A-I+2A-II being the most prominent.

ApoC-III also has been shown to possess the ability to displace apoA-I from HDL but not apoA-II, implying perhaps a greater abundance of apoC-III in LpA-I. However, a prior study reported the prominent presence of apoC-III in LpA-I/A-II (*45*). Our data showed that apoC-III was present in both LpA-I and LpA-I/A-II subfractions and in all the particle sizes. Moreover, our PPP indicated that most particle populations that carried apoC-III contained a single intermolecularly cross-linkable apoC-III molecule, implying these particles may contain only one apoC-III. It was reported that both apoE (*20*, *44*) and apoD (*45*) were more abundant in LpA-I/A-II than in LpA-I. PAGE analysis [Figure 3, lane 1 (LpA-I/A-II)], followed by MALDI-ToF/ToF in our experiments, indicated that apoE and apoD may be predominantly present in the largest subfraction of LpA-I/A-II.

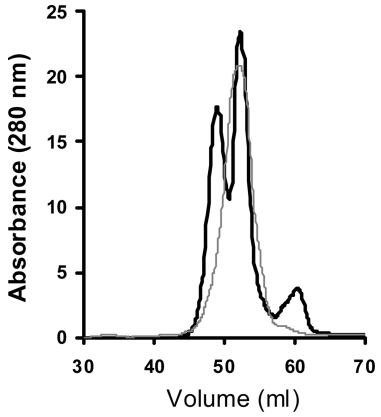

FIGURE 9: Size exclusion chromatography profiles of LpA-I and LpA-I/A-II. LpA-I and LpA-I/A-II were separated on four sizing columns connected in tandem (three Superdex 200 columns followed by a Superose 6 column): LpA-I (black) and LpA-I/A-II (gray).

Particle Size. Separation of LpA-I and LpA-I/A-II on a Superose 6 column setup resulted in very similar elution profiles for both pools (Figure 1). However, PAGE analysis of different subfractions within FPLC profiles indicated different quantized particle sizes for LpA-I, while for LpA-I/A-II, the variation in the particle diameters was smaller (Figures 2 and 5). Hence, we increased the resolution of the chromatographic setup to broaden the elution profile for LpA-I/A-II and attempted to capture different particle sizes. LpA-I and LpA-I/A-II, separated on a set of four sizing columns connected in tandem (0.5 mg, 100 μL), further confirmed that LpA-I/A-II was comprised of particle sizes that had less variability, while LpA-I was clearly composed of at least three distinctly different particle populations (Figure 9). While LpA-I/A-II eluted as a single peak, it overlapped with the midpeak of LpA-I (Figure 9). It was reported that LpA-I and LpA-I/A-II mainly associated with HDL_2 and HDL_3, respectively (*44*, *47*, *49*). Our FPLC data, upon comparison for the particle diameters reported for different density subfractions (*47*), implied that LpA-I/A-II would be associated with the higher-density subfraction HDL_3, while LpA-I covers both the HDL_2 and HDL_3 density range. The average particle diameters of cross-linked subfractions that correspond to three FPLC peaks for LpA-I as seen by native PAGE were 71, 82, and 105 Å, respectively. These diameters agreed closely with the particle diameters of 75−76, 85, and 108 Å, respectively, reported for LpA-I characterized via immunoaffinity chromatographic separation of HDL (*20*, *40*). The reported diameter range for the entire population of LpA-I is 72−129 Å (*47*). Upon separating LpA-I into six subfractions and subjecting them to PAGE analysis with a protein concentration of 1 mg/mL, we were able to visualize a minor population with ~125 Å particle diameters (Figure 5, LpA-I, lanes 1 and 2). However, we were not able to detect distinct particle sizes for LpA-I/A-II even under high-resolution conditions. The PAGE analysis of the FPLC peak in Figure 9 indicated that the average LpA-I/A-II particle size was ~85 Å and the size range of these particles was 85−108 Å (Figure 5). This is in general agreement with a previous report

that captured three particle populations within the range of 78−97 Å for LpA-I/A-II (*47*).

Electron microscopy (EM) measurements performed on LpA-I and LpA-I/A-II main populations, averaging 500 random particles, indicated slightly different average particle diameters for LpA-I (80.9 ± 0.7 Å) and LpA-I/A-II (88.2 ± 0.8 Å). A prior study indicated that LpA-I/A-II particles were smaller (76.5 Å) than LpA-I particles (99.8 Å) (*44*). Notably, the average diameter could be dependent on the abundance of the individual LpA-I particle populations with different diameters. In a situation in which the largest LpA-I particles were the most abundant, as was seen for HDL isolated from women, the average particle size could be shifted to a larger average particle diameter (*46*). It is also worth noting that EM produced less variability in the particle sizes than FPLC and Native PAGE techniques. This could be due to EM capturing only the most abundant particles in each population with nearly similar diameters. The width to length ratio (W/L) ratios of LpA-I (0.90 ± 0.05) and LpA-I/A-II (0.90 ± 0.05) indicated that both types of particles were spherical, a unique piece of evidence that was obtained by EM.

Limitations. The validity of our compositional analyses of HDL subfractions relies on ultracentrifugally isolated total HDL. While some reports have indicated density ultracentrifugation stripping off loosely bound proteins (*45*, *50*), studies have confirmed minimal perturbation to major apolipoproteins in HDL (*20*, *44*), including recovery of more than 90% of apoA-I and 100% apoA-II, under the salt and spin times used in our study (*51*). Data for apoC-III are expected to be similar to those of apoA-II because both apoA-II and apoC-III have the ability to displace apoA-I from HDL as a result of their more lipophilic nature (*43*, *52*). Since apoE seemed to dissociate from HDL up to 50% at least from rodent HDL during ultracentrifugation (*53*), we cautiously report that there could be other subfractions that would contain apoE other than the largest subfraction of LpA-I/A-II. The success of the detection method we used in the study, MALDI-MS, solely relies on the optimal intermolecular cross-linking of all major apolipoproteins within an HDL particle. Because of the presence of apoA-I in larger fractions that escaped intermolecular cross-linking, we could not rule out the presence of LpA-I particles containing more than four apoA-I molecules per particle. Experiments performed on independent batches of HDL confirmed the presence of a fraction of apoA-I in large particles not in a proper orientation for cross-linking with the rest of the proteins. This observation may also indicate protein molecules having moved apart in large particles because of a larger core. A recent study of HDL utilizing surface plasmon resonance spectroscopy revealed a relatively labile pool of apoA-I in HDL particles (*54*). Two different types of apoA-I pools in HDL was also reported on the basis of ultracentrifugation (*51*). Despite optimal cross-linking of small subfractions, our data did not capture the presence of very small HDL particles with perhaps one apoA-I per particle (*55*).

MALDI-MS qualifies as a unique technique for determining molecular stoichiometry of major apolipoproteins in HDL. However, to determine stoichiometry of relatively minor apolipoproteins such as apoE and apoD, further subfractionations followed by specific immunoaffinity isolation of these particles would be necessary. But, limitations due to stripping off of apoE during ultracentrifugation will remain a problem. Use of FPLC in the place of ultracentrifugation could not be an alternative because of the minute amounts of sample that can be obtained. Overlap of the HDL elution profile with other abundant proteins such as albumin and immunoglobulins is another issue (*15*). As reported recently, use of lipid capture reagents for separating HDL, from interfering abundant plasma proteins upon FPLC separations would not work in our experiments, due to difficulty in obtaining native HDL complexes upon this "clean up" step (*15*).

Future Studies. The most important implication of PPPs of different HDL subfractions would be gaining insights into their functional properties. Functional assays could be conducted to assess selective cholesteryl ester uptake (via SR-B1), phospholipid hydrolysis (by endothelial lipase), and triglyceride hydrolysis (by hepatic lipase) and to assess the ability to sequester cholesterol (via ABCG1). Such experiments could yield critical information as to which subfractions of HDL are more active in certain functions and would generate information to correlate functional properties with major apolipoprotein PPPs. The subfraction-specific major enzyme residence and their activity would be another important area of investigation. However, further improvements in gentler techniques for isolating HDL other than ultracentrifugation would be necessary prior to such analyses.

ACKNOWLEDGMENT

We thank Drs. Kerry Anne-Rye and Nataraja Sarma Vaitinadin for their insightful comments and Ms. Cali Smith for her excellent administrative assistance.

SUPPORTING INFORMATION AVAILABLE

Details of the experimental methods. This material is available free of charge via the Internet at http://pubs.acs.org.

REFERENCES

1. Barter, P., Kastelein, J., Nunn, A., and Hobbs, R. (2003) High density lipoproteins (HDLs) and atherosclerosis; the unanswered questions. *Atherosclerosis 168*, 195–211.
2. Ansell, B. J., Watson, K. E., Fogelman, A. M., Navab, M., and Fonarow, G. C. (2005) High-density lipoprotein function recent advances. *J. Am. Coll. Cardiol. 46*, 1792–1798.
3. Navab, M., Ananthramaiah, G. M., Reddy, S. T., Van Lenten, B. J., Ansell, B. J., Fonarow, G. C., Vahabzadeh, K., Hama, S., Hough, G., Kamranpour, N., Berliner, J. A., Lusis, A. J., and Fogelman, A. M. (2004) The oxidation hypothesis of atherogenesis: The role of oxidized phospholipids and HDL. *J. Lipid Res. 45*, 993–1007.
4. Curtiss, L. K., Valenta, D. T., Hime, N. J., and Rye, K. A. (2006) What is so special about apolipoprotein AI in reverse cholesterol transport? *Arterioscler., Thromb., Vasc. Biol. 26*, 12–19.
5. Arakawa, R., Tsujita, M., Iwamoto, N., Ito-Ohsumi, C., Lu, R., Wu, C. A., Shimizu, K., Aotsuka, T., Kanazawa, H., Abe-Dohmae, S., and Yokoyama, S. (2009) Pharmacological inhibition of ABCA1 degradation increases HDL biogenesis and exhibits antiatherogenesis. *J. Lipid Res. 50*, 2299–2305.
6. Zannis, V. I., Chroni, A., and Krieger, M. (2006) Role of apoA-I, ABCA1, LCAT, and SR-BI in the biogenesis of HDL. *J. Mol. Med. 84*, 276–294.
7. Yvan-Charvet, L., Wang, N., and Tall, A. R. (2010) Role of HDL, ABCA1, and ABCG1 transporters in cholesterol efflux and immune responses. *Arterioscler., Thromb., Vasc. Biol. 30*, 139–143.
8. Smith, J. D. (2006) Insight into ABCG1-mediated cholesterol efflux. *Arterioscler., Thromb., Vasc. Biol. 26*, 1198–1200.
9. Asztalos, B. F., Schaefer, E. J., Horvath, K. V., Yamashita, S., Miller, M., Franceschini, G., and Calabresi, L. (2007) Role of LCAT in HDL remodeling: Investigation of LCAT deficiency states. *J. Lipid Res. 48*, 592–599.
10. Klerkx, A. H., El Harchaoui, K., van der Steeg, W. A., Boekholdt, S. M., Stroes, E. S., Kastelein, J. J., and Kuivenhoven, J. A. (2006) Cholesteryl ester transfer protein (CETP) inhibition beyond raising high-density lipoprotein cholesterol levels: pathways by which modulation of CETP activity may alter atherogenesis. *Arterioscler., Thromb., Vasc. Biol. 26*, 706–715.
11. Huuskonen, J., Wohlfahrt, G., Jauhiainen, M., Ehnholm, C., Teleman, O., and Olkkonen, V. M. (1999) Structure and phospholipid transfer

activity of human PLTP: Analysis by molecular modeling and site-directed mutagenesis. *J. Lipid Res. 40*, 1123–1130.
12. Clay, M. A., Newnham, H. H., Forte, T. M., and Barter, P. I. (1992) Cholesteryl ester transfer protein and hepatic lipase activity promote shedding of apo A-I from HDL and subsequent formation of discoidal HDL. *Biochim. Biophys. Acta 1124*, 52–58.
13. Lagrost, L. (1994) Regulation of cholesteryl ester transfer protein (CETP) activity: Review of in vitro and in vivo studies. *Biochim. Biophys. Acta 1215*, 209–236.
14. Vaisar, T., Pennathur, S., Green, P. S., Gharib, S. A., Hoofnagle, A. N., Cheung, M. C., Byun, J., Vuletic, S., Kassim, S., Singh, P., Chea, H., Knopp, R. H., Brunzell, J., Geary, R., Chait, A., Zhao, X. Q., Elkon, K., Marcovina, S., Ridker, P., Oram, J. F., and Heinecke, J. W. (2007) Shotgun proteomics implicates protease inhibition and complement activation in the antiinflammatory properties of HDL. *J. Clin. Invest. 117*, 746–756.
15. Gordon, S. M., Deng, J., Lu, L. J., and Davidson, W. S. (2010) Proteomic characterization of human plasma high density lipoprotein fractionated by gel filtration chromatography. *J. Proteome Res. 9*, 5239–5249.
16. Davidson, W. S., Silva, R. A., Chantepie, S., Lagor, W. R., Chapman, M. J., and Kontush, A. (2009) Proteomic analysis of defined HDL subpopulations reveals particle-specific protein clusters: Relevance to antioxidative function. *Arterioscler., Thromb., Vasc. Biol. 29*, 870–876.
17. Havel, P. J., Goldstein, J. L., and Brown, M. S. (1980) Lipoproteins and Lipid Transport. In The Metabolic Control of Disease (Bondy, P. K., and Rosenburg, L. E., Eds.) pp 393−494, W. B. Saunders, Philadelphia.
18. Bergeron, N., Kotite, L., Verges, M., Blanche, P., Hamilton, R. L., Krauss, R. M., Bensadoun, A., and Havel, R. J. (1998) Lamellar lipoproteins uniquely contribute to hyperlipidemia in mice doubly deficient in apolipoprotein E and hepatic lipase. *Proc. Natl. Acad. Sci. U.S.A. 95*, 15647–15652.
19. Jonas, A. (2002) Lipoprotein Structure. In Biochemistry of Lipids, Lipoproteins and Membranes (Vance, D. E., and Vance, J. E., Eds.) pp 483−504, Elsevier Science, Amsterdam.
20. Cheung, M. C., and Albers, J. J. (1984) Characterization of lipoprotein particles isolated by immunoaffinity chromatography. Particles containing A-I and A-II and particles containing A-I but no A-II. *J. Biol. Chem. 259*, 12201–12209.
21. de Beer, M. C., Durbin, D. M., Cai, L., Mirocha, N., Jonas, A., Webb, N. R., de Beer, F. C., and van der Westhuyzen, D. R. (2001) Apolipoprotein A-II modulates the binding and selective lipid uptake of reconstituted high density lipoprotein by scavenger receptor BI. *J. Biol. Chem. 276*, 15832–15839.
22. Huang, Y., von Eckardstein, A., Wu, S., and Assmann, G. (1995) Cholesterol efflux, cholesterol esterification, and cholesteryl ester transfer by LpA-I and LpA-I/A-II in native plasma. *Arterioscler., Thromb., Vasc. Biol. 15*, 1412–1418.
23. Hime, N. J., Barter, P. J., and Rye, K. A. (1998) The influence of apolipoproteins on the hepatic lipase-mediated hydrolysis of high density lipoprotein phospholipid and triacylglycerol. *J. Biol. Chem. 273*, 27191–27198.
24. Birjmohun, R. S., Dallinga-Thie, G. M., Kuivenhoven, J. A., Stroes, E. S., Otvos, J. D., Wareham, N. J., Luben, R., Kastelein, J. J., Khaw, K. T., and Boekholdt, S. M. (2007) Apolipoprotein A-II is inversely associated with risk of future coronary artery disease. *Circulation 116*, 2029–2035.
25. Roselli della, R. G., Lapolla, A., Sartore, G., Rossetti, C., Zambon, S., Minicuci, N., Crepaldi, G., Fedele, D., and Manzato, E. (2003) Plasma lipoproteins, apoproteins and cardiovascular disease in type 2 diabetic patients. A nine-year follow-up study. *Nutr., Metab. Cardiovasc. Dis. 13*, 46–51.
26. Clay, M. A., Pyle, D. H., Rye, K. A., and Barter, P. J. (2000) Formation of spherical, reconstituted high density lipoproteins containing both apolipoproteins A-I and A-II is mediated by lecithin: cholesterol acyltransferase. *J. Biol. Chem. 275*, 9019–9025.
27. Gillard, B. K., Lin, H. Y., Massey, J. B., and Pownall, H. J. (2009) Apolipoproteins A-I, A-II and E are independently distributed among intracellular and newly secreted HDL of human hepatoma cells. *Biochim. Biophys. Acta 1791*, 1125–1132.
28. de Beer, M. C., van der Westhuyzen, D. R., Whitaker, N. L., Webb, N. R., and de Beer, F. C. (2005) SR-BI-mediated selective lipid uptake segregates apoA-I and apoA-II catabolism. *J. Lipid Res. 46*, 2143–2150.
29. Heuck, C. C., Erbe, I., Frech, K., Lohse, P., and Munscher, G. (1983) Immunonephelometry of apolipoprotein A-II in hyperlipoproteinemic serum. *Clin. Chem. 29*, 1385–1388.
30. Heuck, C. C., Erbe, I., and Flint-Hansen, P. (1983) Immunonephelometric determination of apolipoprotein A-1 in hyperlipoproteinemic serum. *Clin. Chem. 29*, 120–125.
31. Swaney, J. B., and O'Brien, K. (1978) Cross-linking studies of the self-association properties of apo-A-I and apo-A-II from human high density lipoprotein. *J. Biol. Chem. 253*, 7069–7077.
32. Silva, R. A., Huang, R., Morris, J., Fang, J., Gracheva, E. O., Ren, G., Kontush, A., Jerome, W. G., Rye, K. A., and Davidson, W. S. (2008) Structure of apolipoprotein A-I in spherical high density lipoproteins of different sizes. *Proc. Natl. Acad. Sci. U.S.A. 105*, 12176–12181.
33. Bhat, S., Sorci-Thomas, M. G., Alexander, E. T., Samuel, M. P., and Thomas, M. J. (2005) Intermolecular contact between globular N-terminal fold and C-terminal domain of ApoA-I stabilizes its lipid-bound conformation: Studies employing chemical cross-linking and mass spectrometry. *J. Biol. Chem. 280*, 33015–33025.
34. Rye, K. A., Garrety, K. H., and Barter, P. J. (1993) Preparation and characterization of spheroidal, reconstituted high-density lipoproteins with apolipoprotein A-I only or with apolipoprotein A-I and A-II. *Biochim. Biophys. Acta 1167*, 316–325.
35. Massey, J. B., Pownall, H. J., Macha, S., Morris, J., Tubb, M. R., and Silva, R. A. (2009) Mass spectrometric determination of apolipoprotein molecular stoichiometry in reconstituted high density lipoprotein particles. *J. Lipid Res. 50*, 1229–1236.
36. Lund-Katz, S., and Phillips, M. C. (1986) Packing of cholesterol molecules in human low-density lipoprotein. *Biochemistry 25*, 1562–1568.
37. Durbin, D. M., and Jonas, A. (1997) The effect of apolipoprotein A-II on the structure and function of apolipoprotein A-I in a homogeneous reconstituted high density lipoprotein particle. *J. Biol. Chem. 272*, 31333–31339.
38. Rosales, C., Gillard, B. K., Courtney, H. S., Blanco-Vaca, F., and Pownall, H. J. (2009) Apolipoprotein modulation of streptococcal serum opacity factor activity against human plasma high-density lipoproteins. *Biochemistry 48*, 8070–8076.
39. Ito, Y., Breslow, J. L., and Chait, B. T. (1989) Apolipoprotein C-III lacks carbohydrate residues: Use of mass spectrometry to study apolipoprotein structure. *J. Lipid Res. 30*, 1781–1787.
40. Duverger, N., Rader, D., Duchateau, P., Fruchart, J. C., Castro, G., and Brewer, H. B., Jr. (1993) Biochemical characterization of the three major subclasses of lipoprotein A-I preparatively isolated from human plasma. *Biochemistry 32*, 12372–12379.
41. Kontush, A., and Chapman, M. J. (2006) Functionally defective high-density lipoprotein: A new therapeutic target at the crossroads of dyslipidemia, inflammation, and atherosclerosis. *Pharmacol. Rev. 58*, 342–374.
42. Lagocki, P. A., and Scanu, A. M. (1980) In vitro modulation of the apolipoprotein composition of high density lipoprotein. Displacement of apolipoprotein A-I from high density lipoprotein by apolipoprotein A-II. *J. Biol. Chem. 255*, 3701–3706.
43. Edelstein, C., Halari, M., and Scanu, A. M. (1982) On the mechanism of the displacement of apolipoprotein A-I by apolipoprotein A-II from the high density lipoprotein surface. Effect of concentration and molecular forms of apolipoprotein A-II. *J. Biol. Chem. 257*, 7189–7195.
44. James, R. W., Hochstrasser, D., Tissot, J. D., Funk, M., Appel, R., Barja, F., Pellegrini, C., Muller, A. F., and Pometta, D. (1988) Protein heterogeneity of lipoprotein particles containing apolipoprotein A-I without apolipoprotein A-II and apolipoprotein A-I with apolipoprotein A-II isolated from human plasma. *J. Lipid Res. 29*, 1557–1571.
45. Nestruck, A. C., Niedmann, P. D., Wieland, H., and Seidel, D. (1983) Chromatofocusing of human high density lipoproteins and isolation of lipoproteins A and A-I. *Biochim. Biophys. Acta 753*, 65–73.
46. Duverger, N., Rader, D., and Brewer, H. B., Jr. (1994) Distribution of subclasses of HDL containing apoA-I without apoA- II (LpA-I) in normolipidemic men and women. *Arterioscler. Thromb. 14*, 1594–1599.
47. Cheung, M. C., Nichols, A. V., Blanche, P. J., Gong, E. L., Franceschini, G., and Sirtori, C. R. (1988) Characterization of A-I-containing lipoproteins in subjects with A-I Milano variant. *Biochim. Biophys. Acta 960*, 73–82.
48. Jonas, A., Wald, J. H., Toohill, K. L., Krul, E. S., and Kezdy, K. E. (1990) Apolipoprotein A-I structure and lipid properties in homogeneous, reconstituted spherical and discoidal high density lipoproteins. *J. Biol. Chem. 265*, 22123–22129.
49. Atmeh, R. F., Shepherd, J., and Packard, C. J. (1983) Subpopulations of apolipoprotein A-I in human high-density lipoproteins. Their metabolic properties and response to drug therapy. *Biochim. Biophys. Acta 751*, 175–188.

50. McVicar, J. P., Kunitake, S. T., Hamilton, R. L., and Kane, J. P. (1984) Characteristics of human lipoproteins isolated by selected-affinity immunosorption of apolipoprotein A-I. *Proc. Natl. Acad. Sci. U.S.A. 81*, 1356–1360.
51. Kunitake, S. T., and Kane, J. P. (1982) Factors affecting the integrity of high density lipoproteins in the ultracentrifuge. *J. Lipid Res. 23*, 936–940.
52. Pownall, H. J., Pao, Q., Rohde, M., and Gotto, A. M. (1978) Lipoprotein-apoprotein exchange in aqueous systems: Relevance to the occurrence of apoA-I and apoC proteins in a common particle. *Biochem. Biophys. Res. Commun. 85*, 408–414.
53. van't, H. F., and Havel, R. J. (1982) Metabolism of apolipoprotein E in plasma high density lipoproteins from normal and cholesterol-fed rats. *J. Biol. Chem. 257*, 10996–11001.
54. Lund-Katz, S., Nguyen, D., Dhanasekaran, P., Kono, M., Nickel, M., Saito, H., and Phillips, M. C. (2010) Surface plasmon resonance analysis of the mechanism of binding of apoA-I to high density lipoprotein particles. *J. Lipid Res. 51*, 606–617.
55. Atmeh, R. F., and bd Elrazeq, I. O. (2005) Small high density lipoprotein subclasses: Some of their physico-chemical properties and stability in solution. *Acta Biochim. Pol. 52*, 515–525.